

Ligand Effects and Kinetic Investigations of Sterically Accessible 2-Pyridonate Tantalum Complexes for Hydroaminoalkylation

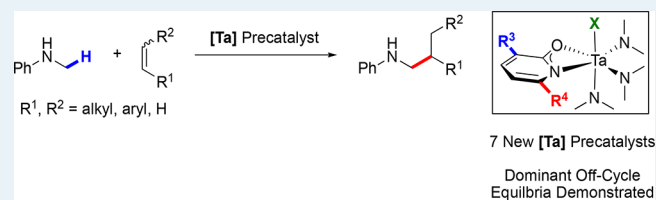
Jason W. Brandt, Eugene Chong, and Laurel L. Schafer*^{ID}

Department of Chemistry, University of British Columbia, 2036 Main Mall, Vancouver, British Columbia, Canada V6T 1Z1

Supporting Information

ABSTRACT: The synthesis of a series of structurally varied pyridonate-supported tantalum amido complexes and their catalytic reactivity in the intermolecular α -alkylation of unprotected secondary amines are described. Both terminal and internal alkenes can undergo this hydroaminoalkylation reaction to give selectively substituted secondary amine products. The reactivity profiles of 3- and 6-substituted pyridonate tantalum complexes, [(2-pyridonate)Ta(NMe₂)₃Cl], and a triflate pyridonate tantalum complex, [(2-pyridonate)Ta(NMe₂)₃OTf], were evaluated to analyze ligand effects. The deprotonation and complexation of commercially available 3-methyl-2-pyridone and 2-pyridone readily yielded effective, catalytically active tantalum complexes, displaying reactivity with both terminal and internal alkene substrates. Kinetic studies and deuterium labeling experiments reveal a complex kinetic profile and provide evidence for off-cycle equilibria that dominate catalytic activity and provide guidance for future catalyst development.

KEYWORDS: hydroaminoalkylation, C–H alkylation, amines, alkenes, tantalum



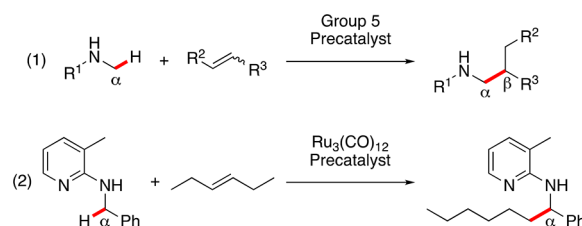
INTRODUCTION

Amine functional groups are ubiquitous throughout chemical industries and are crucial to the function of multiple pharmaceutical, agrochemical, and industrial chemical products.¹ The development of catalytic syntheses of amines as an alternative to traditional stoichiometric methods has found broad applicability from academic syntheses through to industrial applications.

An emerging strategy for the synthesis of selectively substituted amines is the catalytic α -alkylation of amines with alkenes, commonly referred to as hydroaminoalkylation.² This atom-economical approach involves the direct activation of an α -C(sp³)–H bond and its subsequent addition across an alkene unsaturation in an intra- or intermolecular fashion. Employing C–H activation of the amine substrate provides not only an alternative to traditional stoichiometric amine syntheses but also an alternative disconnection strategy to hydroamination,³ Buchwald–Hartwig type,⁴ or Ullman type amine coupling.⁵ The hydroaminoalkylation reaction complements recent advances in the C–H functionalization of simple amine substrates to access value-added substituted amine products.⁶ For example, systems employing photoredox dual catalysis can perform the α -C–H activation and functionalization of amines with anhydrides,^{7a} aryl halides,^{7b,c} cyanoaromatics,^{7f} and nitromethanes.^{7g} Here, catalytic hydroaminoalkylation provides a corresponding coupling alternative to the dual-catalysis approach, instead resulting in alkylation products via the direct hydroalkylation of alkenes.⁸

The majority of research on catalytic hydroaminoalkylation reactions has been focused on early-transition-metal catalyzed variants utilizing Sc,⁹ group 4,¹⁰ and group 5 precatalysts.^{2,11}

Additionally, there are reports utilizing Ru and Ir catalysts.¹² Notably, most Ru and Ir systems require the use of *N*-pyridyl directing groups, with the notable exception of recent work by Krische and co-workers.^{12a,d} While group 5 precatalysts result in almost exclusive formation of the branched, β -alkylated regioisomer (eq 1), late-transition-metal-catalyzed reactions result in the complementary linear isomer, even when internal alkenes are used as substrates (eq 2).^{12i,j}

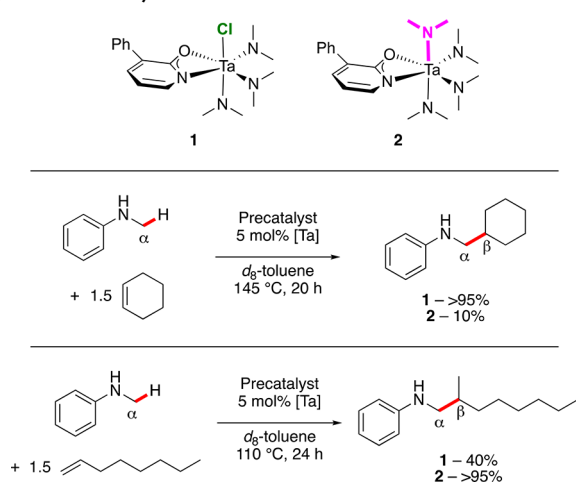


Recently, we reported the synthesis and subsequent catalytic hydroaminoalkylation reactivity of 3-phenyl-2-pyridonate ligated tantalum complexes **1** and **2** (Scheme 1).^{11c} Notably, **1** is the only example of a precatalyst for the hydroaminoalkylation of sterically demanding and unactivated internal alkenes, including *E* and *Z* linear alkenes. The advance in reactivity with internal alkenes offers the ability to create β -substitution with a variety of alkyl and aryl substituents. Intriguingly, complexes **1** and **2** show complementary reactivity toward terminal and internal alkenes (Scheme 1). Complex **1** is the

Received: May 6, 2017

Revised: June 29, 2017

Scheme 1. Recently Reported Ta Precatalysts for Hydroaminoalkylation



only system capable of significant reactivity with internal alkenes while complex **2** shows better reactivity with terminal alkenes over **1**.

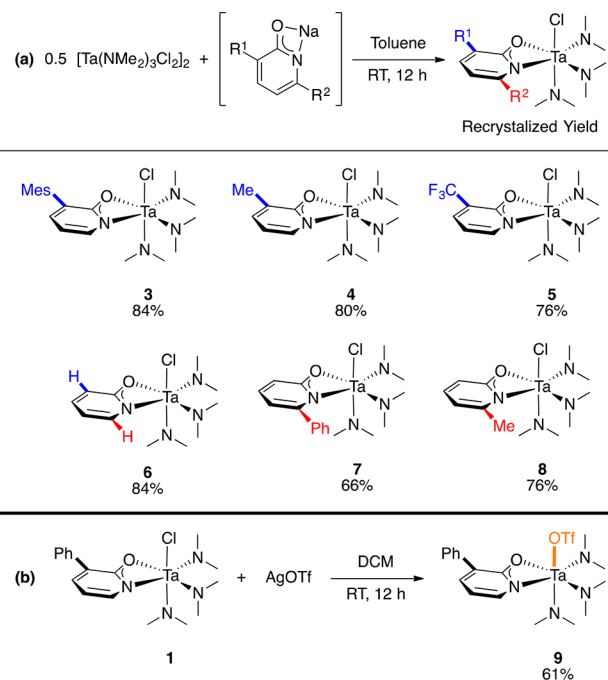
This stark contrast raises questions about the role of the ligand environment of these catalysts. Herein, we describe our efforts toward the synthesis of various precatalysts and evaluation of their catalytic activity toward internal and terminal alkenes, with the aim of developing a catalyst system that can do both effectively. Labeling and kinetic experiments have been used to probe details of the proposed hydroaminoalkylation catalytic cycle. These investigations have revealed that the commercially available 3-methyl-2-pyridone and 2-pyridone can be used as proligands for complexation with tantalum. These readily accessed precatalysts afford high reactivity with terminal alkenes, while retaining high reactivity with internal alkenes. Further insights into catalyst reactivity has shown that these systems have extensive off-cycle equilibria, which limit the interpretation of kinetic data and complicate efforts toward rational catalyst development.

RESULTS AND DISCUSSION

Synthesis and Catalytic Reactivity of Precatalysts. To date, we have disclosed the only catalyst system (**1**) that can effectively mediate intermolecular hydroaminoalkylation of unactivated internal alkenes.^{11c} This unique reactivity profile made use of a 2-pyridonate ligand and built upon established reactivity trends with 1,3-N,O-chelated systems for this reaction.¹³ In an effort to better understand the effect of the pyridonate ligand, a systematic investigation of the steric and electronic properties of 2-pyridonate ligands was undertaken. Given the high reactivity of **1** with internal alkenes, we synthesized a variety of (2-pyridonate)Ta(NMe₂)₂Cl complexes (**3–8**). We have shown previously that substituent effects at the 3- and 6-positions on the pyridonate ligand can dramatically affect intramolecular hydroaminoalkylation.^{10h} In an effort to explore the role of the chloride ligand, we also synthesized complex **9**, featuring an axial triflate ligand.

The synthesis of complexes **3–8** can be achieved via salt metathesis between the sodium 2-pyridonate salt and 1/2 equivalent of dichlorotris(dimethylamido)tantalum dimer (Scheme 2a).^{11c} To prepare complex **9**, complex **1** can be reacted with silver triflate in dichloromethane to produce the desired tantalum triflate analogue (Scheme 2b). All resultant

Scheme 2. Synthesis of Ta Complexes



complexes were prepared in good yield and were fully characterized by ¹H and ¹³C NMR spectroscopy, EI-MS, and EA. In the solution phase, the three inequivalent dimethylamido ligands in all complexes give rise to a single, broad resonance in both the ¹H and ¹³C NMR spectra. This is due to rapid isomerization of the dimethylamido ligands.

Crystals suitable for single-crystal X-ray diffraction of complexes **4**, **5**, and **7** were obtained (Figure 1). Each complex

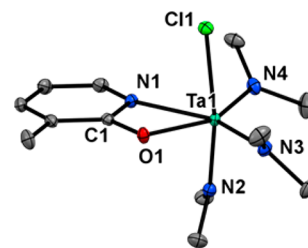


Figure 1. ORTEP representation of complex **4**. Thermal ellipsoids are shown at 50% probability. H atoms are omitted. ORTEP representations of complexes **5** and **7** are included in the Supporting Information.

adopts a distorted-octahedral geometry and shares similarity with the previously reported complex **1**.^{11c} The facial arrangement of the dimethylamido ligands can be attributed to π -bonding effects, as the π -donating amido ligands are all trans to ligands with minimal π -donating ability.¹⁴ A comparison of key bond lengths and angles (Table 1) shows that any substituent-induced variance in the binding of the pyridonate, chloride, or amido is small in the solid state. Of note is the extended Ta–O1 bond lengths in complex **5** and **7** and concomitant shortening of the Ta–Cl bond lengths. Due to the fact that **5** has an electron-withdrawing trifluoromethyl group in the 3-position while **7** has an electron-withdrawing phenyl group in the 6-position, we suggest that this distortion is caused by electron-withdrawing character coupled with steric effects in **7**. However, these

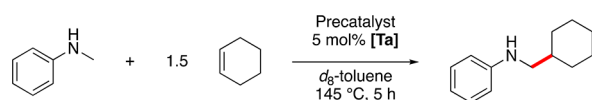
Table 1. Comparison of Key Bond Lengths and Angles of the Solid-State Molecular Structures of 1, 4, 5, and 7

	1 ^{11c}	4	5	7
Ta–N1 (Å)	2.288(4)	2.307(1)	2.295(3)	2.301(1)
Ta–O1 (Å)	2.129(2)	2.122(1)	2.155(2)	2.191(2)
N1–Ta–O1 (deg)	59.30(9)	59.76(5)	59.4(1)	59.13(6)
Ta–Cl (Å)	2.4959(8)	2.4931(5)	2.476(1)	2.4643(6)
av Ta–NMe ₂ (Å)	1.962(8)	1.97(1)	1.97(1)	1.97(1)
Cl–N1 (Å)	1.344(4)	1.364(2)	1.349(4)	1.360(3)
Cl–O1 (Å)	1.298(4)	1.315(2)	1.304(5)	1.302(2)

changes are subtle and we are unable to rule out the possibility that crystal-packing effects dominate the observed metrics. We were unable to obtain crystallographic data for all complexes and have assigned the geometries of the remaining complexes by analogy.

The catalytic activity of these complexes was assessed with the preferred benchmark reactions of *N*-methylaniline with cyclohexene (Scheme 3) and 1-octene (Scheme 4). Complex 1

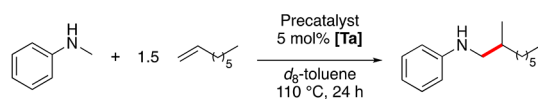
Scheme 3. Catalytic Reactivity with Cyclohexene^a



Complex	1	3	4	5	6	7	8	9
Conversion	32%	36%	39%	13%	33%	5%	15%	8%

^aReaction conditions: *N*-methylaniline (0.5 mmol), cyclohexene (0.75 mmol), [Ta] precatalyst (0.025 mmol), *d*₈-toluene (0.5 mL). Conversion was determined by ¹H NMR spectroscopy. The values are averages of two experiments (see the Supporting Information).

Scheme 4. Catalytic Reactivity with 1-Octene^a



Complex	1	2	4	6	7	8	9
Conversion	40% ^{11c}	>95% ^{11c}	92%	>95%	>95%	>95%	20%

^aReaction conditions: *N*-methylaniline (0.5 mmol), 1-octene (0.75 mmol), [Ta] precatalyst (0.025 mmol), *d*₈-toluene (0.5 mL). Conversion was determined by ¹H NMR spectroscopy. The values are averages of two experiments (see the Supporting Information).

is known to promote the reaction with cyclohexene in >95% conversion (145 °C, 20 h) and with 1-octene in 40% conversion (110 °C, 24 h).^{11c} Reaction times of 5 h (Scheme 3) and 24 h (Scheme 4) were selected to give reaction conversions that would allow for ready comparison of the different ligand environments. Thus, the reported conversions do not represent optimized yields.

Results with cyclohexene reveal that altering the steric parameters at the 3-position (1, 3-phenyl; 3, 3-mesityl; 4, 3-methyl; 6, 3-hydro) of the pyridonate ring results in only minor differences in reactivity. Surprisingly, 5 (3-trifluoromethyl) results in low conversion. Analysis of the ¹⁹F NMR spectrum after the reaction showed various signals in the region of 50–100 ppm. This suggests the formation of Ta–F complexes,¹⁵ via catalyst decomposition. Altering the 6-position (7, 6-phenyl; 8, 3-methyl) of the pyridonate results in a significant decrease

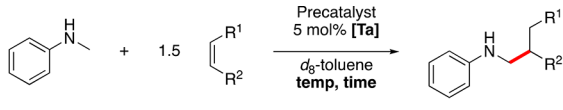
in reactivity. This detrimental effect on catalytic performance is proposed to be due to the added steric congestion at the metal center, thereby hindering reactivity with the sterically demanding internal alkene substrate. The use of 9 results in poor conversion. In this case, no Ta–F complexes could be observed by ¹⁹F NMR spectroscopy at the end of the catalytic reaction.

Using a terminal alkene, 1-octene, as a substrate provides significantly different results (Scheme 4). A marked increase in conversion occurs when the steric parameter is reduced in the 3-position of the pyridonate (4 and 6). Intriguingly, increasing the steric parameter of the pyridonate in the 6-position (7 and 8) also provides high conversion with this less sterically demanding terminal alkene substrate. As with the cyclohexene substrate, the triflate complex 9 provided disappointing reactivity with 1-octene.

Complexes 4 and 6 are the first examples of highly active catalysts for both internal and terminal alkenes. These complexes offer a minimal increase over our previously reported complex 1 for reactivity with cyclohexene. However, 4 and 6 are comparable to 2 and are significantly better than 1 for reactions with 1-octene. An attractive advantage to 4 and 6 is the fact that the 2-pyridone proligands are commercially available and inexpensive.

To further elucidate the general reactivity of 4 and 6, additional reactions with various alkene substrates were completed (Scheme 5). By reduction of the reaction time to 20 h with 1-octene (entry 1), the difference in reactivity between 4 and 6 could be better observed. Gratifyingly, 6 produces 86% yield (>95% conversion), while complex 4 is slightly less active (63% yield). Reactivity with different internal alkenes (entries 2–6) shows that complex 4 is more broadly useful than 6. With cyclohexene (entry 2) and cycloheptene (entry 3), 4 provides yields of 81% and 93%, respectively, in 4 h less than it takes 1 to provide comparable yields (88% and 95%, respectively). Complex 4 provides slightly less conversion in 24 h than 1 (83% vs 92%) with (*Z*)-methylstyrene substrate (entry 5) but, more significantly, reduced yields with (*E*)-3-hexene (entry 4) and (1*S*)- β -pinene (entry 6): 21% and 23% reductions in yield, respectively. Complexes 4 and 6 both offer regioselectivity comparable with that of (*Z*)-methylstyrene (entry 5) and diastereoselectivity comparable with that of (1*S*)- β -pinene (entry 6), in comparison to the reported complex 1.

Complex 4 is a readily accessible, broadly reactive hydro-aminoalkylation precatalyst and is the first catalyst system offering excellent reactivity profiles with both internal and terminal alkenes. However, efforts to optimize reaction yields for specific amine/alkene substrate combinations demanded empirical screening, and no reliable reactivity trends could be determined. To improve our predictive ability to select and design optimized catalyst systems, mechanistic investigations were undertaken.

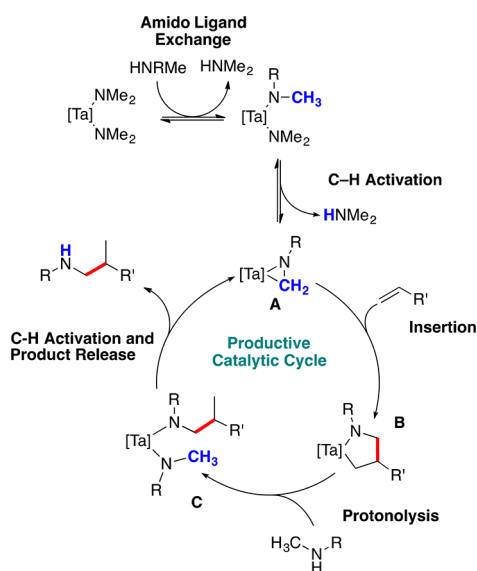
Scheme 5. Comparative Hydroaminoalkylation Reactivity of 4 and 6^e


Entry	Products	Conds.	4	6
1		110 °C 20 h	63%	86%
2		145 °C 16 h	81%	44%
3		130 °C 16 h	93%	95%
4		145 °C 44 h	58%	31%
5		145 °C 24 h	83% (3.0:1) ^{a,b}	29% (3.7:1) ^{a,b}
6		145 °C 54 h	32% (20:1) ^{c,d}	14% (>20:1) ^{c,d}

^aMajor regioisomer shown. ^bRatio determined by ¹H NMR analysis. ^cMajor diastereomer shown. ^dRatio determined by UHPLC analysis. ^eReaction conditions: *N*-methylaniline (0.5 mmol), alkene (0.75 mmol), [Ta] precatalyst (0.025 mmol), ferrocene (0.05–0.11 mmol), *d*₈-toluene (0.5 mL). Yield was determined by ¹H NMR spectroscopy with ferrocene internal standard. Values are averages of two experiments (see the Supporting Information).

Mechanistic Investigations. We and others have proposed a simplified catalytic cycle for hydroaminoalkylation as presented in Scheme 6.^{11h,q,r} Entry into the active catalytic

Scheme 6. Proposed Catalytic Cycle for Early-Transition-Metal-Catalyzed Hydroaminoalkylation



cycle occurs via an amine exchange to ligate the substrate amine to the metal center, followed by C–H activation via hydrogen abstraction by an adjacent amido ligand to give tantalazaaziridine A. Insertion of the alkene into the reactive Ta–C bond forms metallacycle B. Subsequent protonolysis of the Ta–C bond with incoming amine substrate generates C. Another C–H activation event allows for release of the significantly larger product amine, releasing steric strain around the metal center and regenerating the reactive tantalazaaziridine moiety. Kinetic mechanistic research by Hultsch and co-workers on a tantalum BINOLate complex did not conclusively identify the rate-determining step(s) for their system.^{11h} Their work does show that the rate-determining step is influenced by amine substrate.

We previously proposed that the introduction of the planar pyridonate and the chloro ligands (complex 1) reduces the steric constraints for the insertion step (A to B) and/or protonolysis step (B to C), allowing for productive catalysis with sterically demanding internal alkenes.^{11c} These two steps both involve high steric congestion of the metal center, where complexes of the type [(2-pyridonate)Ta(NMe₂)₃Cl] provide the necessary steric relief for catalytic turnover. The decreased reactivity shown by 6-phenyl (7) and 6-methyl (8) with cyclohexene can be explained by the increased steric constraints imparted by 6-substituted 2-pyridonates on the metal center.

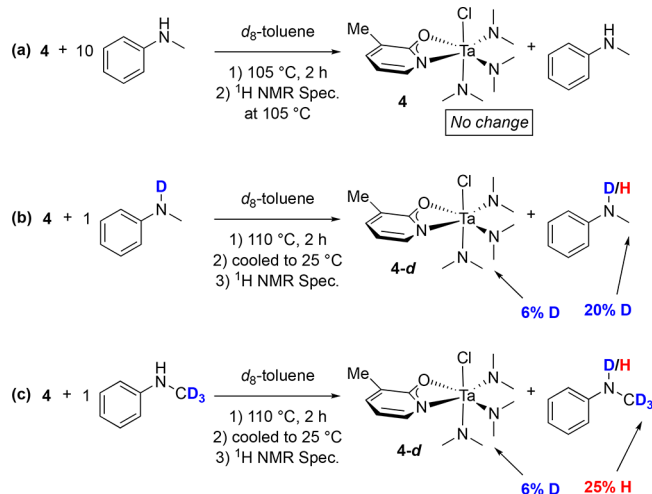
When utilizing the less sterically demanding terminal alkene substrate 1-octene, complex 1 shows markedly reduced reactivity in comparison to 2. We have previously proposed that the overall steric congestion at the metal center in 2 (effected by the replacement of the chloro ligand with an amido ligand) is required for effective catalytic turnover when employing sterically less demanding terminal alkenes.^{11c} Unlike the simple picture employed in Scheme 6, we suggest the equilibrium between off-cycle and on-cycle tantalum species lies heavily toward the off-cycle species (vide infra). This has the effect of lowering the reaction rate, as the concentration of on-cycle species is low at any time during the reaction. Additionally, these off-cycle species are involved in multiple equilibria with rapid exchange of all amines present in solution. The increased congestion at the metal center in 2, as well as in 6-substituted 2-pyridone complexes 7 and 8, encourages product amine to be released from the metal center, resulting in a higher concentration of substrate amine bound as an amido ligand. We posit that this higher concentration of active species results in the observed increase in reactivity.

Intriguingly, the most sterically accessible pyridonate complexes 4 (3-methyl) and 6 (3,6-dihydro) provide high reactivity for both internal alkenes and 1-octene. In the context of the above rationalizations, the reactivity of 4 and 6 is unexpected. With internal alkenes, complex 1 and 4 provide similar reactivity (with modest improvements over 6) with substrate-dependent variations in reactivity. This suggests the 3-substitution of the 2-pyridonate ligand has limited effects with sterically demanding substrates. A major departure occurs with 1-octene substrate. Complex 6 exhibits higher reactivity than 4, and both demonstrate reactivity comparable to that of 2, despite lacking substituents that would impart increased steric crowding at the metal center. Both 4 and 6 offer improved conversion over that of complex 1. Most likely, complexes 4 and 6 alter the turnover-limiting step(s) in a more complex way than is rationalized above.

Investigations into Precatalyst Activation and Off-Cycle Equilibria. Initial investigations focused on probing the amine exchange reaction during the precatalyst activation. In an

effort to observe precatalyst activation, both amido ligand exchange and the C–H activation reactions, we heated a mixture of **4** with *N*-methylaniline at the catalytically relevant temperature of 110 °C (Scheme 7a). We expected to observe

Scheme 7. Deuterium Scrambling Experiment^a



^aDeuterium incorporation determined by $^1\text{H NMR}$ spectroscopy and deuteration confirmed by $^2\text{H NMR}$ spectroscopy.

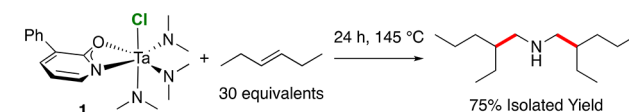
the formation of a complex with one or more anilido ligands and concomitant release of dimethylamine. This may have also resulted in the formation of *N*-phenyl tantalazaaziridine in situ. Interestingly, not only is there no evidence of tantalazaaziridine formation but also there is no decomposition of **4**, no consumption of *N*-methylaniline, and no release of dimethylamine when observations are made at elevated temperatures in the NMR spectrometer with in situ monitoring. This shows that the sterically less demanding dimethylamido ligands (in comparison to *N*-methylanilido) are favored as ligands for this tantalum complex.

Previous reports from our group demonstrated that tantalazaaziridine formation could be promoted by increased steric demand at the metal center, in one case by the addition of a second N,O-chelated amidate ligand.^{11o} Further, Hultzs et al. propose that C–H activation is facile and reversible in sterically encumbered BINOLate tantalum catalysts.^{11h} We were curious to see if we could observe facile C–H activation in our systems despite having significantly decreased steric bulk at the metal center.

A mixture of complex **4** with an excess of *N-d-N*-methylaniline was heated at 110 °C for 2 h (Scheme 7b). Here the deuterium of the amine group washes into the methyl groups of the precatalyst dimethylamido ligands and into the methyl group of the *N*-methylaniline substrate, as observed by $^2\text{H NMR}$ at 3.51 and 2.30 ppm, respectively. Furthermore, a mixture of complex **4** with *N*-(methyl-*d*₃)aniline heated to 110 °C for 2 h results in hydrogen being incorporated into the methyl group of the previously deuterated *N*-(methyl-*d*₃)aniline. These results reveal that amido ligand exchange and C–H activation pathways are rapid and reversible at catalytically relevant temperatures. Additionally, the experiments presented in Scheme 7 conclusively show that an equilibrium is present between **4** (precatalyst) and *N*-methylaniline and that this equilibrium strongly favors **4** (to the limit of detection of $^1\text{H NMR}$ spectroscopy).

All of the reactions in Scheme 7 have been carried out in the absence of alkene substrate. Previous work from our group has shown that the dimethylamido ligands of the precatalyst are not innocent during catalytic reactions, as they also undergo alkylation via hydroaminoalkylation.^{11d,16} Furthermore, complex **1** in the presence of excess 3-hexene and no exogenous amine results in high yields of dialkylated dimethylamine (Scheme 8).¹⁷ Given the aforementioned facile and reversible

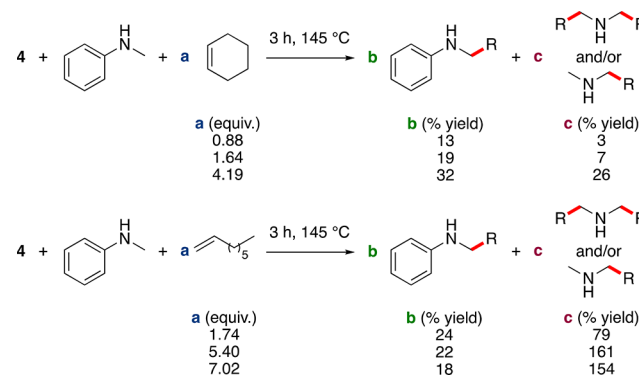
Scheme 8. Isolation of Dialkylated Byproduct^a



^aYield relative to **1**, which contains 3 equiv of dimethylamine.

amido ligand exchange and C–H activation reactions with **4**, we questioned how dimethylamido ligands/free dimethylamine may affect the desired catalytic alkylation of *N*-methylaniline. To this end, we set up a series of stoichiometric reactions with complex **4**, *N*-methylaniline, and increasing amounts of either cyclohexene or 1-octene (Scheme 9). These reaction mixtures were then heated to 145 °C (cyclohexene) or 110 °C (1-octene) for 3 h.

Scheme 9. Stoichiometric Experiments with Variable Alkene Amounts Monitoring Relative Amounts of Product and Byproduct Formation at Partial Conversion^a

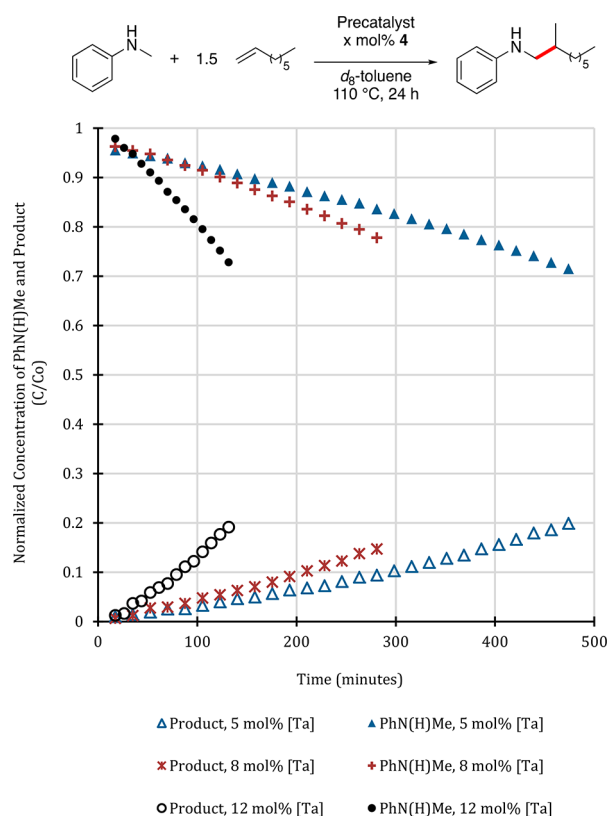


^aNote: remainder of mass balance is from that retained as unreacted starting materials. Equivalents for *a* values and yields for *b* and *c* values (reported relative to initial amount of *N*-methylaniline) are calculated by $^1\text{H NMR}$ spectroscopy with 1,3,5-trimethoxybenzene as an internal standard.

Generally, we observe a mixture of both products, suggesting that the rates of functionalization of *N*-methylaniline and dimethylamine are comparable and are in competition with each other for activation in the catalytic cycle. Furthermore, substrate-dependent equilibria appear to dominate, as reactions with 1-octene yield significantly more alkylated dimethylamine byproducts in comparison to reactions with cyclohexene substrates. We also observe that, as alkene equivalents increase, the amount of byproduct formation increases relative to the amounts of product. These experiments show that complex equilibria are at play in these catalytic reactions and amido ligand exchange allows for significant amounts of both product and byproduct formation at the initial stages of the hydroaminoalkylation reaction.

Further evidence of such equilibria is presented in Scheme 10. The catalytic reaction of *N*-methylaniline and 1-octene with

Scheme 10. Hydroaminoalkylation Reaction Monitoring with 5, 8, and 12 mol % of [Ta] Precatalyst 4^a

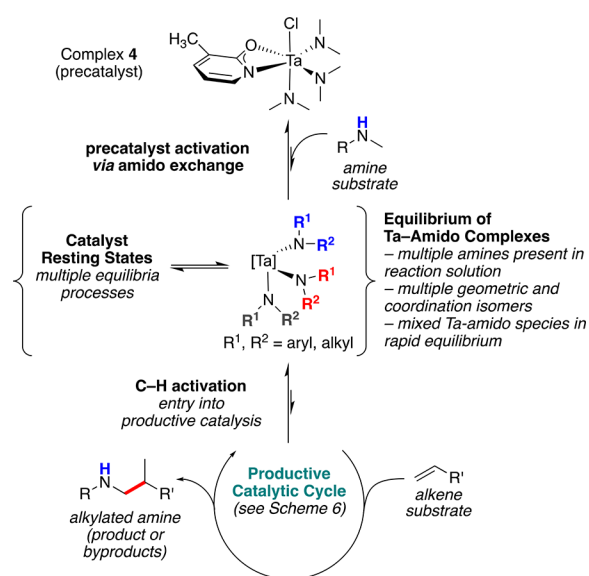


^aReaction conditions: *N*-methylaniline (0.5 mmol), 1-octene (0.75 mmol), [Ta] precatalyst (0.025, 0.04, or 0.06 mmol), 1,3,5-trimethoxybenzene (0.17 mmol), *d*₆-toluene (0.5 mL). See the Supporting Information for experimental details. Plot of average of two runs. See Chart S1 in the Supporting Information for a plot of nonaveraged data.

4 can be monitored by ¹H NMR spectroscopy at 105 °C.¹⁸ Product formation could be observed by the appearance of the diagnostic *o*-H proton signal at 6.41 ppm, with the concomitant consumption of starting *N*-methylaniline, as observed by the disappearance of the peak at 6.33 ppm. Due to the long reaction times, the reaction monitoring was limited to the first approximately 20% conversion with 5, 8, and 12 mol % of precatalyst 4 (Scheme 10).

Notably, this system displays an increasing rate with time, resulting in curved profiles observed for both product formation and starting material consumption. The observed profile is present in reactions with 5, 8, and 12 mol % of precatalyst loading, suggesting that increased catalyst loading does not alter this behavior. This profile is consistent with an extended induction period. Induction periods are associated with the activation of precatalyst and are ideally short lived. In this system, there is a period of increasing rate that continues to evolve up to 20% conversion. Unfortunately, these changing rates prevent quantitative kinetic assessments. However, the assembly of the data presented in Schemes 7–10 leads us to propose that the observed extended induction period is the result of extensive off-cycle equilibria between various tantalum amido species (Scheme 11). The equilibrium studies between

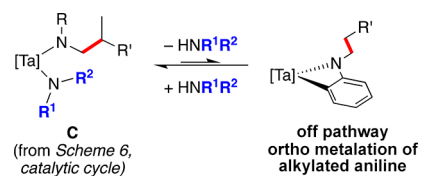
Scheme 11. Resting State Equilibria



complex 4 and *N*-methylaniline define that the equilibrium lies heavily toward a combination of amido ligands that minimizes steric crowding of the metal center. The slowly increasing rates are consistent with the alkylation of dimethylamido ligands, resulting in the formation of more sterically demanding amine byproducts. These sterically demanding products in turn favor the formation of less sterically demanding *N*-methylanilido tantalum species. Thus, there is an observable increase in the rate of hydroaminoalkylation of *N*-methylaniline. The equilibria between numerous and variable resting state species limit the formation of catalytically active tantalaziridine. We propose that these complicated and evolving equilibria result in the low observed turnover frequency of catalysis.

Finally, other reports of hydroaminoalkylation have observed reversible sp²-hybridized C–H bond activation using deuterium labeling experiments.^{11h,q,16} This is proposed to proceed via the formation of the cyclometalated intermediate shown in Scheme 12. To determine if sp²-hybridized C–H activation is occurring

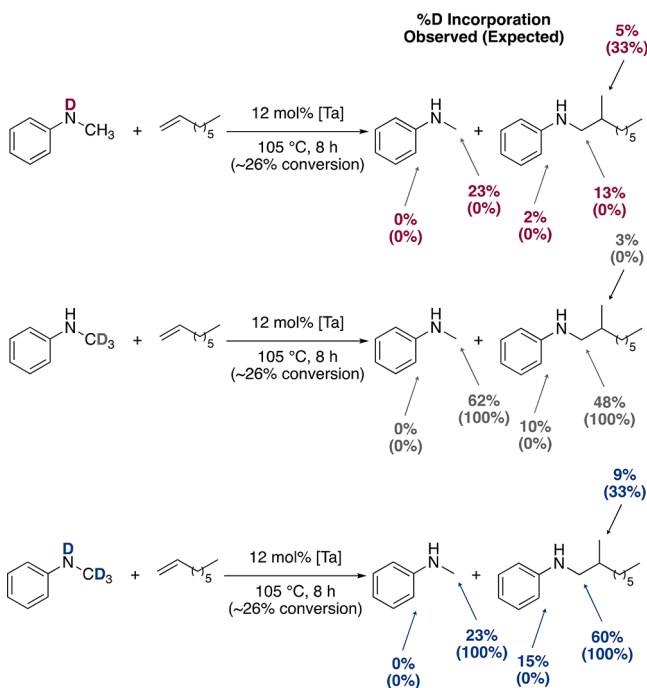
Scheme 12. Ortho-Deuteration Off-Pathway Equilibrium



with precatalyst 4, we have also monitored the reaction with variably deuterated aniline substrates using 12 mol % of precatalyst at 105 °C by ¹H NMR spectroscopy until ~26% conversion of starting *N*-methylaniline (see Chart S2 in the Supporting Information for a plot of results).

After monitoring, one reaction with each deuterated aniline was quenched and subjected to column chromatography. Both the starting *N*-methylaniline and the alkylation aniline product were isolated. Deuterium incorporation was confirmed by ²D NMR spectroscopy and quantified with ¹H NMR spectroscopy. The results of deuterium quantification are summarized in Scheme 13.

Scheme 13. Analysis of Deuterium Incorporation into Product and Byproduct Aniline after Partial Catalytic Conversion with Variably Deuterated Aniline Substrates^a



^aReaction conditions: *N*-methylaniline (0.5 mmol), 1-octene (0.75 mmol), [Ta] precatalyst (0.06 mmol), 1,3,5-trimethoxybenzene (0.17 mmol), *d*₈-toluene (0.5 mL). See the Supporting Information for experimental details. Deuterium incorporation determined by ¹H NMR spectroscopy and deuteration confirmed by ²H NMR spectroscopy.

The results of these experiments are also consistent with many off-cycle equilibria, as there are significant deviations in deuterium incorporation from the expected results on the basis of the mechanistic proposal presented in Scheme 6. The observation of deuterium in the ortho position of the phenyl ring of the final product confirms that both *sp*³ and *sp*² C–H bond activation is occurring; however, productive catalysis only proceeds via the tantalaziridine reactive intermediate.

Our analysis of starting *N*-methylaniline represents the first report of analysis of this starting material after being subjected to catalytic hydroaminoalkylation conditions. Interestingly, the unreacted starting *N*-methylaniline does not reversibly incorporate deuterium in the ortho position. This demonstrates that *sp*³-hybridized C–H (or C–D) activation is more favorable than *sp*² C–H activation. However, once the methyl group of the starting material is converted to the methylene group in the product, subsequent *sp*³-hybridized C–H (or C–D) activation is hindered, allowing for C–H activation of the ortho position to become energetically relevant. The observation that methyl C(*sp*³)–H activation is favored over methylene C(*sp*³)–H activation is consistent with previous examples in the literature. Multiple examples of hydroaminoalkylation from our group and others have observed decreased catalytic activity with non-*N*-methyl substrates. Substrates of this type remain a challenge and have been rarely reported.^{11e,f,o,p} Also of note, Hultsch et al. report scrambling of PhN(H)CD₂CD₃ when it is heated alone with 2 mol % of a binolate tantalum catalyst.^{11h} In their report they observe significant deuterium incorporation into the ortho position of

the aryl ring and loss of deuterium from the methylene (α to the amine) position, consistent with our results presented here.

CONCLUSION

Our investigations into the ligand effects of the 2-pyridonate ligands on complexes of the type [(2-pyridonate)Ta(NMe₂)₃Cl] resulted in the identification of readily accessed catalyst systems that can be generated from a commercially available 3-methyl-2-pyridonate (4) or the simple 2-pyridonate (6) as ligand. Complexes 4 and 6 are the first examples of hydroaminoalkylation catalysts that offer promising reactivity with both internal and terminal alkene substrates. Efforts to understand how ligand substitution affects catalyst activity resulted in the identification of complicating off-cycle equilibria that include (1) readily reversible trans-amination and C–H activation reactions in precatalyst activation, (2) unwanted byproduct formation resulting from alkylation of the dimethylamido ligands of the precatalyst, (3) complex mixtures of catalyst resting states resulting from the generation of multiple Ta amido complexes in situ, and (4) the observation that C–H activation can occur at both *sp*³- and *sp*²-hybridized C–H bonds. Considered together, these factors play a significant role in limiting the generation of on-cycle tantalum species, thereby severely limiting catalytic turnover. Ongoing work is focused on new ligand environments that avoid the use of dimethylamido ligands to both increase the concentration of productive on-cycle tantalum species and increase the efficiency of catalytic hydroaminoalkylation.

ASSOCIATED CONTENT

Supporting Information

The Supporting Information is available free of charge on the ACS Publications website at DOI: 10.1021/acscatal.7b01486.

Experimental procedures, compound characterization data (¹H, ¹³C, and ¹⁹F NMR spectra), and X-ray data (PDF)

Crystallographic data (CIF)

Crystallographic data (CIF)

Crystallographic data (CIF)

AUTHOR INFORMATION

Corresponding Author

*E-mail for L.L.S.: Schafer@chem.ubc.ca.

ORCID

Laurel L. Schafer: 0000-0003-0354-2377

Notes

The authors declare no competing financial interest.

ACKNOWLEDGMENTS

The authors thank the NSERC for financial support of this work. J.W.B. and E.C. thank the NSERC for postgraduate scholarships. This research was undertaken, in part, thanks to funding from the Canada Research Chairs program. We thank Scott Ryken (UBC) and Damon Gilmour (UBC) for the collection of single-crystal X-ray data.

REFERENCES

- Lawrence, S. A. *Amines: Synthesis, Properties and Applications*; Cambridge University Press: Cambridge, U.K., 2004.
- (a) Chong, E.; Garcia, P.; Schafer, L. L. *Synthesis* **2014**, *46*, 2884–2896. (b) Roesky, P. W. *Angew. Chem., Int. Ed.* **2009**, *48*, 4892–4894.

- (3) Schafer, L. L.; Yim, J. C.-H.; Yonson, N. Transition-Metal-Catalyzed Hydroamination Reactions. In *Metal-Catalyzed Cross-Coupling Reactions and More*; Meijere, A. d., Bräse, S., Oestreich, M., Eds.; Wiley-VCH: Weinheim, Germany, 2014; pp 1135–1258.
- (4) (a) Maiti, D.; Fors, B. P.; Henderson, J. L.; Nakamura, Y.; Buchwald, S. L. *Chem. Sci.* **2011**, *2*, 57–68. (b) Paradies, J. Palladium-Catalyzed Aromatic Carbon–Nitrogen Bond Formation. In *Metal-Catalyzed Cross-Coupling Reactions and More*; Meijere, A. d., Bräse, S., Oestreich, M., Eds.; Wiley-VCH: Weinheim, Germany, 2014; pp 995–1066.
- (5) Sambiagio, C.; Marsden, S. P.; Blacker, A. J.; McGowan, P. C. *Chem. Soc. Rev.* **2014**, *43*, 3525–3550.
- (6) (a) Xu, Y.; Young, M. C.; Wang, C.; Magness, D. M.; Dong, G. *Angew. Chem., Int. Ed.* **2016**, *55*, 9084–9087. (b) Wu, Y.; Chen, Y. Q.; Liu, T.; Eastgate, M. D.; Yu, J. Q. *J. Am. Chem. Soc.* **2016**, *138*, 14554–14557. (c) Topczewski, J. J.; Cabrera, P. J.; Saper, N. I.; Sanford, M. S. *Nature* **2016**, *531*, 220–224. (d) Liu, Y.; Ge, H. *Nat. Chem.* **2017**, *9*, 26–32. (e) Lee, M.; Sanford, M. S. *J. Am. Chem. Soc.* **2015**, *137*, 12796–12799. (f) He, C.; Gaunt, M. J. *Angew. Chem., Int. Ed.* **2015**, *54*, 15840–15844. (g) Calleja, J.; Pla, D.; Gorman, T. W.; Domingo, V.; Haffemayer, B.; Gaunt, M. J. *Nat. Chem.* **2015**, *7*, 1009–1016. (h) McNally, A.; Haffemayer, B.; Collins, B. S.; Gaunt, M. J. *Nature* **2014**, *510*, 129–133.
- (7) (a) Joe, C. L.; Doyle, A. G. *Angew. Chem., Int. Ed.* **2016**, *55*, 4040–4043. (b) Ahneman, D. T.; Doyle, A. G. *Chem. Sci.* **2016**, *7*, 7002–7006. (c) Zuo, Z.; Ahneman, D. T.; Chu, L.; Terrett, J. A.; Doyle, A. G.; MacMillan, D. W. *Science* **2014**, *345*, 437–440. (d) Prier, C. K.; Rankic, D. A.; MacMillan, D. W. *Chem. Rev.* **2013**, *113*, 5322–5363. (e) Tucker, J. W.; Stephenson, C. R. *J. Org. Chem.* **2012**, *77*, 1617–1622. (f) McNally, A.; Prier, C. K.; MacMillan, D. W. *Science* **2011**, *334*, 1114–1117. (g) Condie, A. G.; Gonzalez-Gomez, J. C.; Stephenson, C. R. *J. Am. Chem. Soc.* **2010**, *132*, 1464–1465.
- (8) Dong, Z.; Ren, Z.; Thompson, S. J.; Xu, Y.; Dong, G. *Chem. Rev.* **2017**, *117*, 9333.
- (9) Nako, A. E.; Oyamada, J.; Nishiura, M.; Hou, Z. M. *Chem. Sci.* **2016**, *7*, 6429–6434.
- (10) (a) Manßen, M.; Lauterbach, N.; Dörfler, J.; Schmidtman, M.; Saak, W.; Doye, S.; Beckhaus, R. *Angew. Chem., Int. Ed.* **2015**, *54*, 4383–4387. (b) Hamzaoui, B.; Pelletier, J. D. A.; El Eter, M.; Chen, Y.; Abou-Hamad, E.; Basset, J. M. *Adv. Synth. Catal.* **2015**, *357*, 3148–3154. (c) Dörfler, J.; Preuß, T.; Brahms, C.; Scheuer, D.; Doye, S. *Dalton Trans.* **2015**, *44*, 12149–12168. (d) Dörfler, J.; Bytyqi, B.; Hüller, S.; Mann, N. M.; Brahms, C.; Schmidtman, M.; Doye, S. *Adv. Synth. Catal.* **2015**, *357*, 2265–2276. (e) Dörfler, J.; Preuss, T.; Schischko, A.; Schmidtman, M.; Doye, S. *Angew. Chem., Int. Ed.* **2014**, *53*, 7918–7922. (f) Preuss, T.; Saak, W.; Doye, S. *Chem. - Eur. J.* **2013**, *19*, 3833–3837. (g) Dörfler, J.; Doye, S. *Angew. Chem., Int. Ed.* **2013**, *52*, 1806–1809. (h) Chong, E.; Schafer, L. L. *Org. Lett.* **2013**, *15*, 6002–6005. (i) Chong, E.; Qayyum, S.; Schafer, L. L.; Kempe, R. *Organometallics* **2013**, *32*, 1858–1865. (j) Jaspers, D.; Saak, W.; Doye, S. *Synlett* **2012**, *23*, 2098–2102. (k) Prochnow, I.; Zark, P.; Muller, T.; Doye, S. *Angew. Chem., Int. Ed.* **2011**, *50*, 6401–6405. (l) Prochnow, I.; Kubiak, R.; Frey, O. N.; Beckhaus, R.; Doye, S. *ChemCatChem* **2009**, *1*, 162–172. (m) Kubiak, R.; Prochnow, I.; Doye, S. *Angew. Chem., Int. Ed.* **2009**, *48*, 1153–1156. (n) Bexrud, J. A.; Eisenberger, P.; Leitch, D. C.; Payne, P. R.; Schafer, L. L. *J. Am. Chem. Soc.* **2009**, *131*, 2116–2118.
- (11) (a) Hamzaoui, B.; Pelletier, J. D. A.; Abou-Hamad, E.; Chen, Y.; El Eter, M.; Chermak, E.; Cavallo, L.; Basset, J.-M. *Chem. - Eur. J.* **2016**, *22*, 3000–3008. (b) Dörfler, J.; Doye, S. *Eur. J. Org. Chem.* **2014**, *2014*, 2790–2797. (c) Chong, E.; Brandt, J. W.; Schafer, L. L. *J. Am. Chem. Soc.* **2014**, *136*, 10898–10901. (d) Zhang, Z.; Hamel, J.-D.; Schafer, L. L. *Chem. - Eur. J.* **2013**, *19*, 8751–8754. (e) Payne, P. R.; Garcia, P.; Eisenberger, P.; Yim, J. C.-H.; Schafer, L. L. *Org. Lett.* **2013**, *15*, 2182–2185. (f) Garcia, P.; Payne, P. R.; Chong, E.; Webster, R. L.; Barron, B. J.; Behrle, A. C.; Schmidt, J. A. R.; Schafer, L. L. *Tetrahedron* **2013**, *69*, 5737–5743. (g) Garcia, P.; Lau, Y. Y.; Perry, M. R.; Schafer, L. L. *Angew. Chem., Int. Ed.* **2013**, *52*, 9144–9148. (h) Reznichenko, A. L.; Hultsch, K. C. *J. Am. Chem. Soc.* **2012**, *134*, 3300–3311.
- (i) Lauzon, J. M. P.; Schafer, L. L. *Dalton Trans.* **2012**, *41*, 11539.
- (j) Zhang, F.; Song, H.; Zi, G. *Dalton Trans.* **2011**, *40*, 1547.
- (k) Reznichenko, A. L.; Emge, T. J.; Audörsch, S.; Klauber, E. G.; Hultsch, K. C.; Schmidt, B. *Organometallics* **2011**, *30*, 921–924.
- (l) Zi, G.; Zhang, F.; Song, H. *Chem. Commun.* **2010**, *46*, 6296.
- (m) Eisenberger, P.; Schafer, L. L. *Pure Appl. Chem.* **2010**, *82*, 1503–1515. (n) Segawa, Y. *Yuki Gosei Kagaku Kyokaiishi* **2009**, *67*, 843–844.
- (o) Eisenberger, P.; Ayinla, R. O.; Lauzon, J. M. P.; Schafer, L. L. *Angew. Chem., Int. Ed.* **2009**, *48*, 8361–8365. (p) Herzog, S. B.; Hartwig, J. F. *J. Am. Chem. Soc.* **2008**, *130*, 14940–14941. (q) Herzog, S. B.; Hartwig, J. F. *J. Am. Chem. Soc.* **2007**, *129*, 6690–6691. (r) Nugent, W. A.; Ovenall, D. W.; Holmes, S. J. *Organometallics* **1983**, *2*, 161–162. (s) Clerici, M. G.; Maspero, F. *Synthesis* **1980**, *1980*, 305–306.
- (12) (a) Chen, T. Y.; Tsutsumi, R.; Montgomery, T. P.; Volchkov, I.; Krische, M. J. *J. Am. Chem. Soc.* **2015**, *137*, 1798–1801. (b) Schinkel, M.; Wang, L.; Bielefeld, K.; Ackermann, L. *Org. Lett.* **2014**, *16*, 1876–1879. (c) Lahm, G.; Opatz, T. *Org. Lett.* **2014**, *16*, 4201–4203. (d) Schmitt, D. C.; Lee, J.; Dechert-Schmitt, A. M.; Yamaguchi, E.; Krische, M. J. *Chem. Commun.* **2013**, *49*, 6096–6098. (e) Pan, S. G.; Shibata, T. *ACS Catal.* **2013**, *3*, 704–712. (f) Pan, S.; Matsuo, Y.; Endo, K.; Shibata, T. *Tetrahedron* **2012**, *68*, 9009–9015. (g) Bergman, S. D.; Storr, T. E.; Prokopcova, H.; Aelvoet, K.; Diels, G.; Meerpoel, L.; Maes, B. U. *Chem. - Eur. J.* **2012**, *18*, 10393–10398. (h) Pan, S.; Endo, K.; Shibata, T. *Org. Lett.* **2011**, *13*, 4692–4695. (i) Chatani, N.; Asami, T.; Yorimitsu, S.; Ikeda, T.; Kakiuchi, F.; Murai, S. *J. Am. Chem. Soc.* **2001**, *123*, 10935–10941. (j) Jun, C.-H. *Chem. Commun.* **1998**, 1405–1406.
- (13) Ryken, S. A.; Schafer, L. L. *Acc. Chem. Res.* **2015**, *48*, 2576–2586.
- (14) Thomson, R. K.; Zahariev, F. E.; Zhang, Z.; Patrick, B. O.; Wang, Y. A.; Schafer, L. L. *Inorg. Chem.* **2005**, *44*, 8680–8689.
- (15) Marchetti, F.; Pampaloni, G.; Zacchini, S. *J. Fluorine Chem.* **2010**, *131*, 21–28.
- (16) Lauzon, J. M. P.; Eisenberger, P.; Roşca, S.-C.; Schafer, L. L. *ACS Catal.* **2017**, DOI: 10.1021/acscatal.7b01293.
- (17) Chong, E. Early Transition Metal Complexes of Pyridine Derivatives: Applications in the Catalytic Synthesis of Amines and N-Heterocycles. Ph.D. Dissertation, University of British Columbia, Vancouver, BC, Canada, 2014.
- (18) Multiple attempts to monitor the reaction at 145 °C using the internal olefin cyclohexene were unsuccessful. Attempts to alter the reaction conditions by scale or by vessel resulted in inconsistent and poor yields (ca. <10%). Attempts to use d^{10} -*o*-xylenes and monitor the reaction at 140 °C by ^1H NMR spectroscopy resulted in poor yields (ca. <10%) for similar reaction times. We believe these results are due to unquantified pressure effects.